ACS Catalysis

pubs.acs.org/acscatalysis Research Article

Remote γ-C(sp^3)−H Alkylation of Aliphatic Carboxamides via an Unexpected Regiodetermining Pd Migration Process: Reaction Development and Mechanistic Study

Ya Li,[§] Pan Zhang,[§] Yue-Jin Liu, Zhi-Xiang Yu,* and Bing-Feng Shi*

Cite This: *ACS Catal.* 2020, 10, 8212−8222 Read Online

ACCESS | Metrics & More | Article Recommendations | Supporting Information

ABSTRACT: In the presence of accessible β-C−H bonds, γ-C−H activation of saturated aliphatic carboxamides remains unresolved because β-C−H activation is kinetically favored. This is almost a dogma in the development of C−H activation reactions. Here we report a strategy to change this dogma, as we have found that a Pd-catalyzed, ligand-enabled remote γ-alkylation of saturated aliphatic carboxamides can be realized in the presence of more accessible β-C−H bonds by using strained bicyclic alkenes as the coupling partners. Density functional theory calculations and experiments suggested that the realization of the present reaction is due to a change in the regiodetermining step from commonly encountered irreversible C−H activations, which are reversible here, to an unexpected Pd migration process, which is regiodetermining. This is a new strategy to achieve γ-C−H activation, compared with the previous strategy, making γ-C−H activation both the turnover- and regiodetermining step.

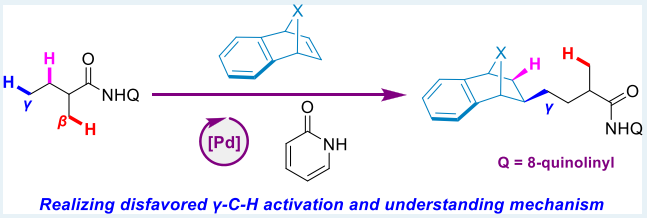

Realizing disfavored γ-C-H activation and understanding mechanism

KEYWORDS: *C−H activation, site-selective, remote selectivity, ligand promotion, 1,4-Pd migration*

INTRODUCTION

Pd-catalyzed aliphatic C−H functionalization has become a powerful synthetic tool for rapidly increasing molecular complexity and diversity.[1−13] To be synthetically useful, strategies that selectively cleave one single C−H bond among many chemically similar ones present in organic molecules must be developed.[14−17] Directing groups (DGs) are typically used to achieve this goal by positioning the palladium catalyst near a target C−H bond and enabling the selective cleavage via cyclopalladation.[18] Among various functionalities capable of assisting C−H activation, carboxylic acids and their derivatives are attractive because of their ubiquity and synthetic versatility.[18] Nevertheless, most carboxyl-directed aliphatic C−H activation reactions proceed through a kinetically favored five-membered palladacycle, thus enabling functionalization at the β-position (Scheme 1a). The direct functionalization of aliphatic C−H bonds at the remote γ-position remains a formidable challenge because of the difficulty of forming the kinetically less favored six-membered palladacycle. To date, only scattered examples of γ-C(sp^3)−H functionalizations have been reported. Corey,[19] Chatani,[20] Chen,[21,22] Shi,[23] and Maiti[24−27] have elegantly demonstrated γ-C(sp^3)−H functionalizations assisted by strong bidentate amide DGs.[6−9,28] The Yu group pioneered Pd(II)-catalyzed γ-C−H olefination, carbonylation, and arylation using the combination of a quinoline-based ligand and a weakly coordinating amide DG.[29,30] Recently, Maiti and our group also independently reported *N*-protected amino acid assisted γ-C(sp^3)−H arylation of free aliphatic acid.[31,32] It should be noted that *these reactions are limited to carboxamides without primary or secondary β-C−H bonds* (Scheme 1b). Further advances in this field should concentrate on selective functionalization of γ-methyl C−H bonds of aliphatic carboxylic acids and their derivatives in the presence of β-methyl and/or β-methylene C−H bonds. We think that this can be realized by the use of two strategies.

It is believed that the inherent β-selectivity is governed kinetically because β-C−H activation is more geometrically accessible than γ-C−H activation. The C−H activation steps are followed by fast β-C−Pd bond transformation and functionalization. Consequently, C−H activation becomes both the rate-determining and regiodetermining step. Therefore, strategy I for realizing γ-C−H activation in the presence of β-C−H bonds is to make γ-C−H activation more favorable than β-C−H activation by designing new DGs. Yu and co-workers designed new strained DGs that were assembled to generate the geometrically favored six-membered palladacycles in order to realize strategy I for remote C−H functionalizations of amines and alcohols.[33,34] Those DGs are not applicable to aliphatic carboxylic acids and their derivatives.

Received: May 6, 2020
Revised: May 27, 2020
Published: June 11, 2020

https://dx.doi.org/10.1021/acscatal.0c02025
ACS Catal. 2020, 10, 8212−8222

Scheme 1. Pd-Catalyzed C(sp^3)−H Functionalization of Aliphatic Carboxamides

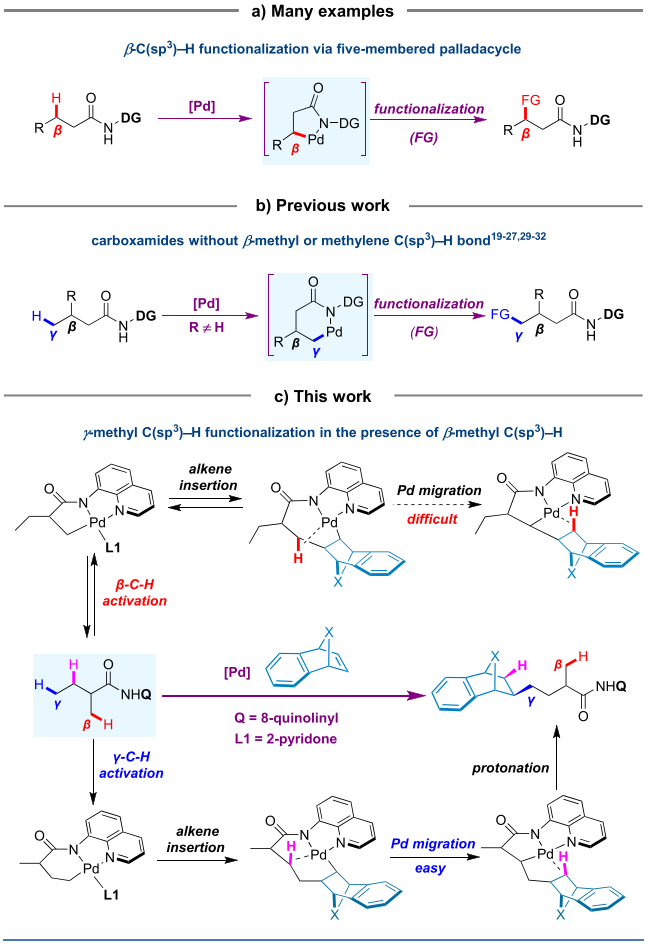

Following our previous reports,[35,36] we propose another strategy, here indicated as strategy II, to turn the site selectivity to the γ-C−H bond: changing the regiodetermining step to a step after the C−H activations, which must be reversible. In other words, even though γ-C−H activation is disfavored over β-C−H activation, one of the steps after the reversible C−H activations could favor the pathway of γ-C−H activation. This can be easily understood by the Curtin−Hammett principle.[37] Guided by this strategy, we have observed the first Pd-catalyzed γ-C(sp^3)−H alkylation of saturated aliphatic carboxamides via kinetically less favorable γ-C−H activation in the presence of more accessible β-C−H bonds (Scheme 1c).[38] This reaction has a broad scope. We have also carried out a mechanistic investigation and found that the selectivity-determining step of the whole process has been switched from the C−H activation step, which still favors β-C−H activation over γ-C−H activation, to an unprecedented Pd migration that favors γ-C−H alkylation. We present here both experimental and density functional theory (DFT) studies of this discovery. Successful utilization and mechanistic understanding of this strategy by us and other groups may provide another alternative way to realize other remote C−H activation reactions.

RESULTS AND DISCUSSION

Optimization of the Reaction Conditions. Our initial studies proceeded with the reaction of 2-methyl-*N*-(quinolin-8-yl)butanamide (**1a**) and 7-oxabenzonorbornadiene (**2a**).[39−43] We were pleased to observe that the γ-alkylation product **3aa** was obtained in 16% yield in the presence of 1-AdCOOH (Table S3). The yield could be further improved to 35% when sterically more bulky 2,2-diethylbutanoic acid was used (Table S6). However, extensive screening of various other conditions and carboxylic acids failed to improve the yield (Tables S1−S5). Encouraged by Yu's seminal work on the use of 2-pyridone-based ligands as strongly coordinating X-type ligands to promote C−H activation,[44−49] we embarked on screening this kind of ligand. To our delight, the yield increased to 50% when 2-pyridone (**L1**) was used. Pd(dba)$_2$ was found to be slightly more effective than Pd(OAc)$_2$. We hypothesized that the 2-pyridone played a dual role (1) as a σ donor through the pyridyl nitrogen to promote the in situ oxidation of Pd(0) to Pd(II) by air[50,51] and (2) as a stronger X-type ligand coordinated with Pd(II) to accelerate C−H activation. Also, the in situ oxidation of Pd(dba)$_2$ obviates the introduction of excess OAc$^-$.[52] When K$_2$HPO$_4$ and NaTFA were used and the temperature was increased to 120 °C, the ^{1}H NMR yield improved to 72% (Table 1; TCP = 1,2,3-trichloropropane). Next, a wide range of 2-pyridone-type ligands (**L1**−**L18**) were investigated, and **L1** was proved to be the optimal one. The yield was significantly decreased in the absence of a 2-pyridone ligand (<5%). Moving the hydroxyl group to other positions (**L20**−**L22**) or protecting the hydroxyl or amide in the ligand (**L23** and **L24**) resulted in complete loss of reactivity. The reaction proceeded with good mass balance with respect to the carboxamide substrate, and the formation of other side products, such as those resulting from β-alkylation, cyclopropanation,[53] and ring-opening of oxabicycles,[54] were not observed.

Table 1. Evaluation of 2-Pyridone-Type Ligands[a,b]

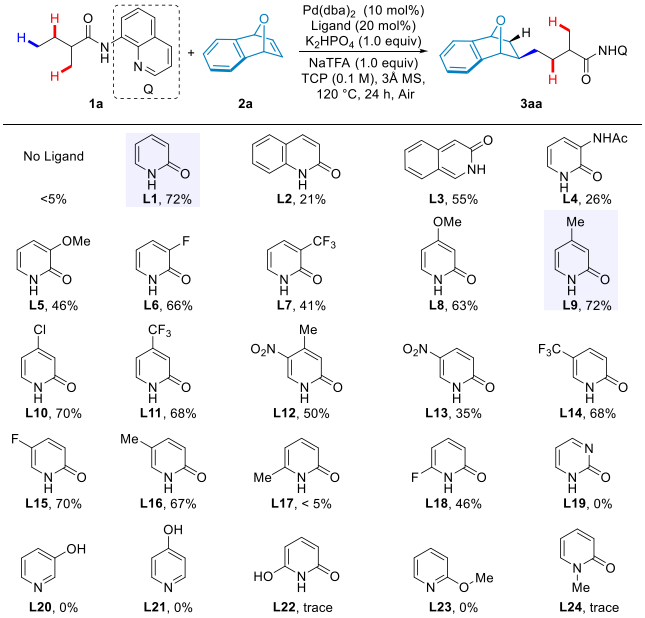

[a]Reaction conditions: **1a** (0.10 mmol), **2a** (0.12 mmol), Pd(dba)$_2$ (10 mol %), ligand (20 mol %), K$_2$HPO$_4$ (0.10 mmol), NaTFA (0.10 mmol), and 3 Å MS (40 mg) in 1,2,3-trichloropropane (TCP) (1 mL) at 120 °C for 24 h under air. [b]Yields were determined by ^{1}H NMR spectroscopy using CH$_2$Br$_2$ as an internal standard.

Study of the Reaction Scope of the Substrates. With the optimized conditions in hand, we explored the scope of aliphatic carboxamides bearing accessible β-C(sp^3)−H bonds

https://dx.doi.org/10.1021/acscatal.0c02025
ACS Catal. 2020, 10, 8212−8222

(Table 2). This protocol is compatible with carboxamides bearing one, two, or three β-methyl groups (**1a**–**c**), and 2,3,3-trimethybutanamide (**1c**) gave a higher yield (74%), presumably due to the *gem*-dimethyl effect. Carboxamides **1d** and **1e**, a couple of diastereoisomers, gave distinct reactivity: the trans isomer afforded the alkylation product **3da** in 48% yield, while the cis isomer showed a complete loss of reactivity. This can be explained by the strong steric repulsion between the Me and Ph groups in the resulting six-membered palladacycle **INT**-*trans*-**3e**.[34] Moreover, carboxamides containing various more accessible β-methylene C–H bonds were also compatible with this protocol (**1f**–**j**), exclusively affording the desired γ-alkylated products in moderate to good yields (44-75%). Carboxamide **3k** with no accessible β-C–H bond, which was generally used in previous reports,[24−27] gave the γ-alkylated product in 32% yield, as expected.

Different strained bicyclic alkenes were also examined (Table 3). A variety of 7-oxabenzonorbornadienes (**2a**–**j**) reacted efficiently with **1a** to afford the corresponding γ-alkylation products **3aa**–**aj**. Generally speaking, alkenes bearing electron-withdrawing groups (**2e**–**g**) on the phenyl ring reacted slightly better than those with electron-donating substituents (**2c** and **2d**). Halogens (fluoro, **2e**; chloro, **2g**; bromo, **2f** and **2i**) were well-tolerated. Bridgehead-substituted 7-oxabenzonorbornadiene (**2j**) also reacted, albeit with relatively low yield, probably because of the increased steric hindrance. Notably, the reaction also proceeded well with 7-azabenzonorbornadienes (**2k**–**n**), benzonorbornadiene (**2o**), and 7-oxabornadiene (**2p**) to give the corresponding γ-alkylation products exclusively. It is noteworthy that γ-alkylation occurred exclusively and no other side products related to β-C–H functionalization were observed in any reactions that we examined.

Table 2. Scope of Aliphatic Carboxamides[a]

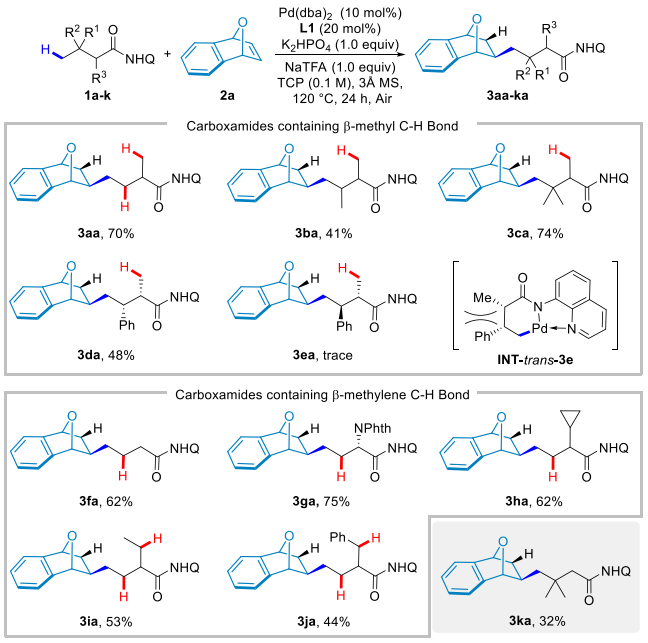

[a]Reaction conditions: **1** (0.10 mmol), **2a** (0.12 mmol), $Pd(dba)_2$ (10 mol %), ligand (20 mol %), K_2HPO_4 (0.10 mmol), NaTFA (0.10 mmol), and 3 Å MS (40 mg) in TCP (1 mL) at 120 °C for 24 h under air.

Table 3. Scope of Strained Bicyclic Alkenes[a]

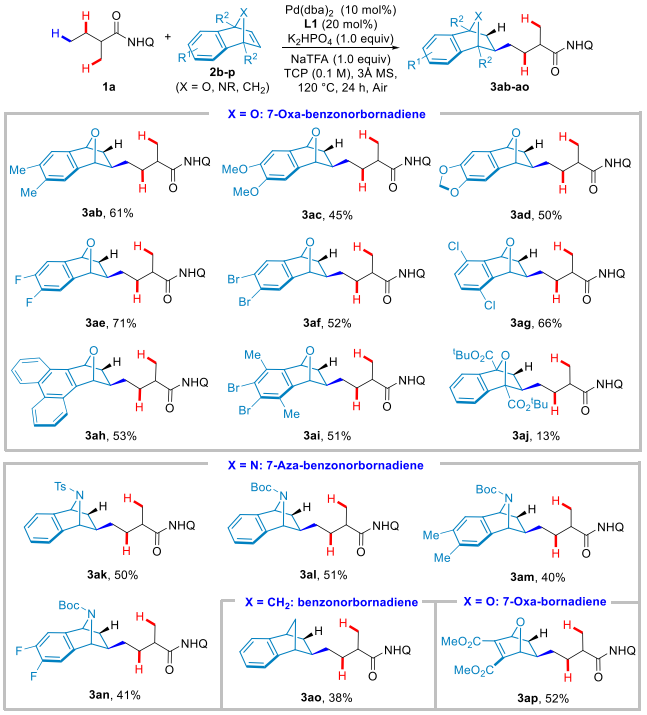

[a]Reaction conditions: **1a** (0.10 mmol), **2** (0.12 mmol), $Pd(dba)_2$ (10 mol %), ligand (20 mol %), K_2HPO_4 (0.10 mmol), NaTFA (0.10 mmol), and 3 Å MS (40 mg) in TCP (1 mL) at 120 °C for 24 h under air.

Sequential C(sp^3)–H Functionalization. The unique remote selectivity provided us an opportunity to sequentially functionalize γ- and β-C(sp^3)–H bonds of carboxamide **1a** in two steps (Table 4). After the site-selective γ-C–H alkylation, various well-developed β-C(sp^3)–H functionalization reactions, including silylation,[55] methoxycarbonylation,[56] alkylation,[57] alkenylation,[58] alkynylation,[58] and arylation,[59] were conducted,

Table 4. Sequential C(sp^3)–H Functionalization of 1a

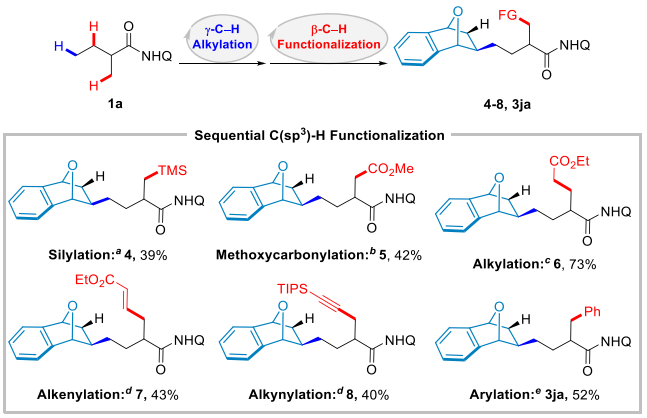

[a]$Pd(OAc)_2$, $(SiMe_3)_2$, *rac*-BINOL-PO_2H, Ag_2CO_3, $NaHCO_3$, LiOAc, toluene, air, 125 °C, 24 h. [b]$Pd(OAc)_2$, $ClCO_2Me$, Ag_2CO_3, Na_3PO_4, toluene, air, 120 °C, 24 h. [c]$Pd(OAc)_2$, ICH_2CO_2Et, $(BnO)_2PO_2H$, Ag_2CO_3, ^{t}AmylOH, air, 110 °C, 24 h. [d]$Pd(OAc)_2$, (*E*)-ICHCH-CO_2Me or BrCCSi(^{i}Pr)$_3$, AgTFA, TCE/H_2O, air, 65 °C, 24 h. [e]$Pd(OAc)_2$, PhI, $AgBF_4$, ^{t}BuOH, N_2, 120 °C, 24 h.

https://dx.doi.org/10.1021/acscatal.0c02025
ACS Catal. 2020, 10, 8212−8222

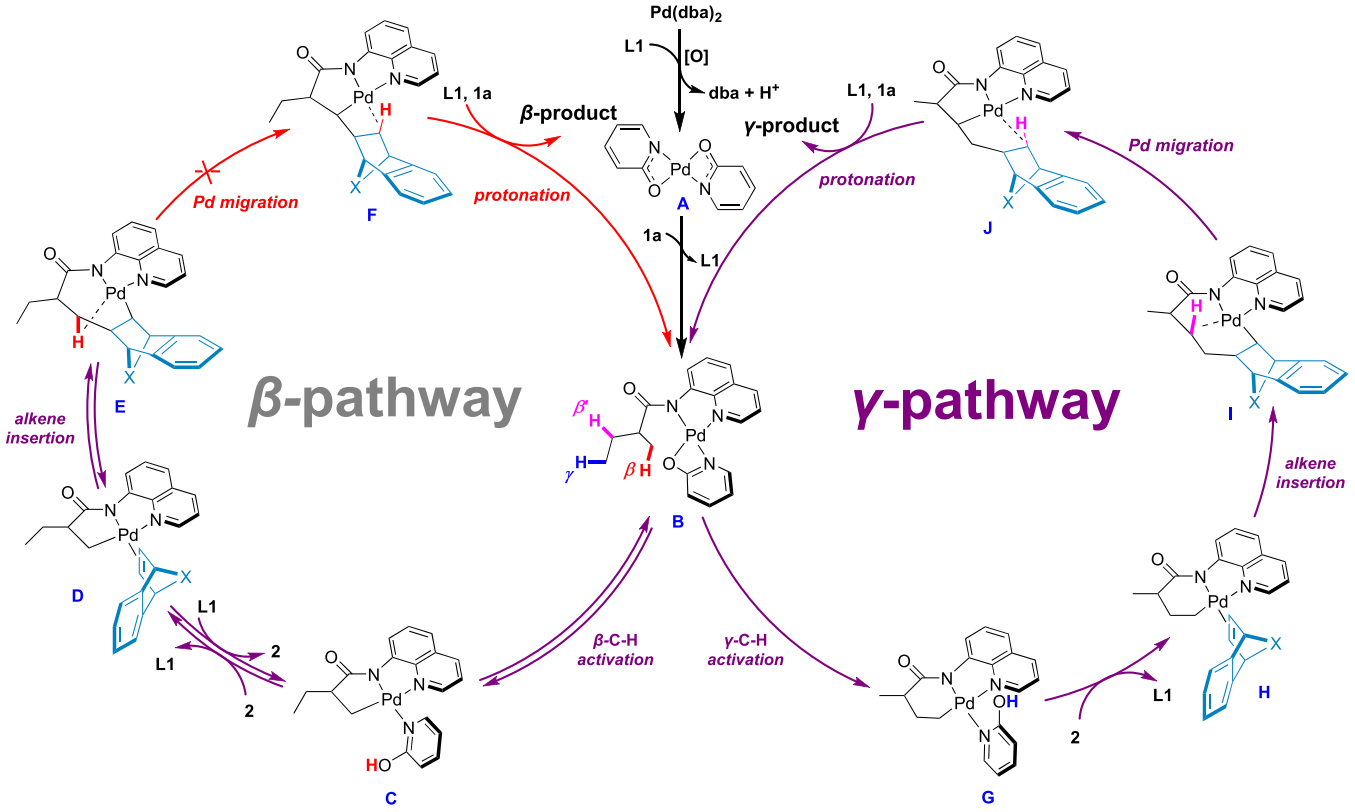

Figure 1. Proposed mechanism.

affording carboxamides with various functionalities (**4**−**8** and **3ja**).

Study of the Reaction Mechanism. We carried out both experimental and DFT investigations of the mechanism of the present γ-alkylation, and the finalized mechanism is given in Figure 1. We propose that $Pd(dba)_2$ is first oxidized by air to form the Pd(II) species, which then forms intermediate **A** with two **L1** ligands.[50] The substrate **1a** is then deprotonated and forms intermediate **B**, liberating one **L1** ligand. Intermediate **B** can then undergo either β-C−H activation to give intermediate **C** or γ-C−H activation to give intermediate **G**, both via a concerted metalation−deprotonation (CMD) mechanism,[60] where the **L1** ligand's oxygen can abstract the C−H bonds in the substrate in both pathways. Then ligand exchanges between **2** (alkene) and **L1** give intermediates **D** and **H** in the β and γ pathways, respectively. Alkene insertion in these two pathways gives **E** and **I**, respectively. Previously, Chen and coworkers proposed that these two intermediates could then be protonated directly to give the final alkylation products.[61] However, our DFT calculations and experiments excluded these processes (see later discussions). Instead, we propose that there is a Pd migration[61] to give **F** and **J** in both pathways. Finally, protonation of **F** and **J** gives the β- and γ-alkylation products. Our mechanistic studies suggested that the formation of **C** and **D** in the β pathway is preferred kinetically compared with **G** and **H** in the γ pathway, but the Pd migration is difficult in the β pathway compared to the γ pathway. Consequently, the γ pathway is preferred (strategy II). In one word, the present reaction has the preference for γ over β because of the change in the selectivity-determining step from C−H activation, which favors the β pathway and has been found in many reactions, to Pd migation, which is unprecedented and here favors the γ pathway. Therefore, in the following, we present our mechanistic studies to elucidate this selectivity.

Let us first discuss the β pathway, which is shown in Figure 2. **1a** and **2a** were used as the model substates for the calculations. This pathway starts with CMD of the β-C−H bond of **B** (generation of **B** is shown in the Supporting Information (SI)) via **TS1** to give intermediate **C**, with an activation free energy of 15.8 kcal/mol. Ligand exchange between alkene **2a** and **L1**, which is almost a thermodynamically neutral process, gives intermediate **IN1**, which then undergoes alkene insertion to give intermediate **IN2**. The alkene insertion is endergonic by 17.4 kcal/mol. (The diastereoselectivity of the alkene insertion step does not affect the reaction selectivity, as discussed in the SI.)

According to a previous report,[61] **IN2** could be protonated directly to give the final product. This possible process is shown in Scheme 2. Coordination of **L1** to **IN2** affords **IN12**, which subsequently undergoes amide N protonation easily, leading to **IN13** via **TS11**. Then the second coordination of **L1** occurs to give **IN14**. Unfortunately, C protonation of **IN14** (via **TS12**) is very difficult, requiring 36.2 kcal/mol (from **IN14** to **TS12**). Another direct protonation pathway in which the Pd−C bond of **IN2** is first protonated was also considered. However, this process is more difficult (see the SI for details). Thus, we proposed another pathway to give the β product by Pd migration via **TS3** and then protonation. In other words, **IN2** would undergo Pd migration to give **IN3**, which then undergoes intramolecular protonation by the **L1** ligand's hydroxy group. Unfortunately, the Pd migration is also disfavored because this needs 32.2 kcal/mol (from **C** to **TS3**, the Pd migration transition state). Therefore, both direct protonation and Pd migration in the β pathway are kinetically disfavored compared with the γ pathway (see the later discussion). More discussion of alkene insertion and Pd migration will be given in the analysis of the γ

https://dx.doi.org/10.1021/acscatal.0c02025
ACS Catal. 2020, 10, 8212−8222

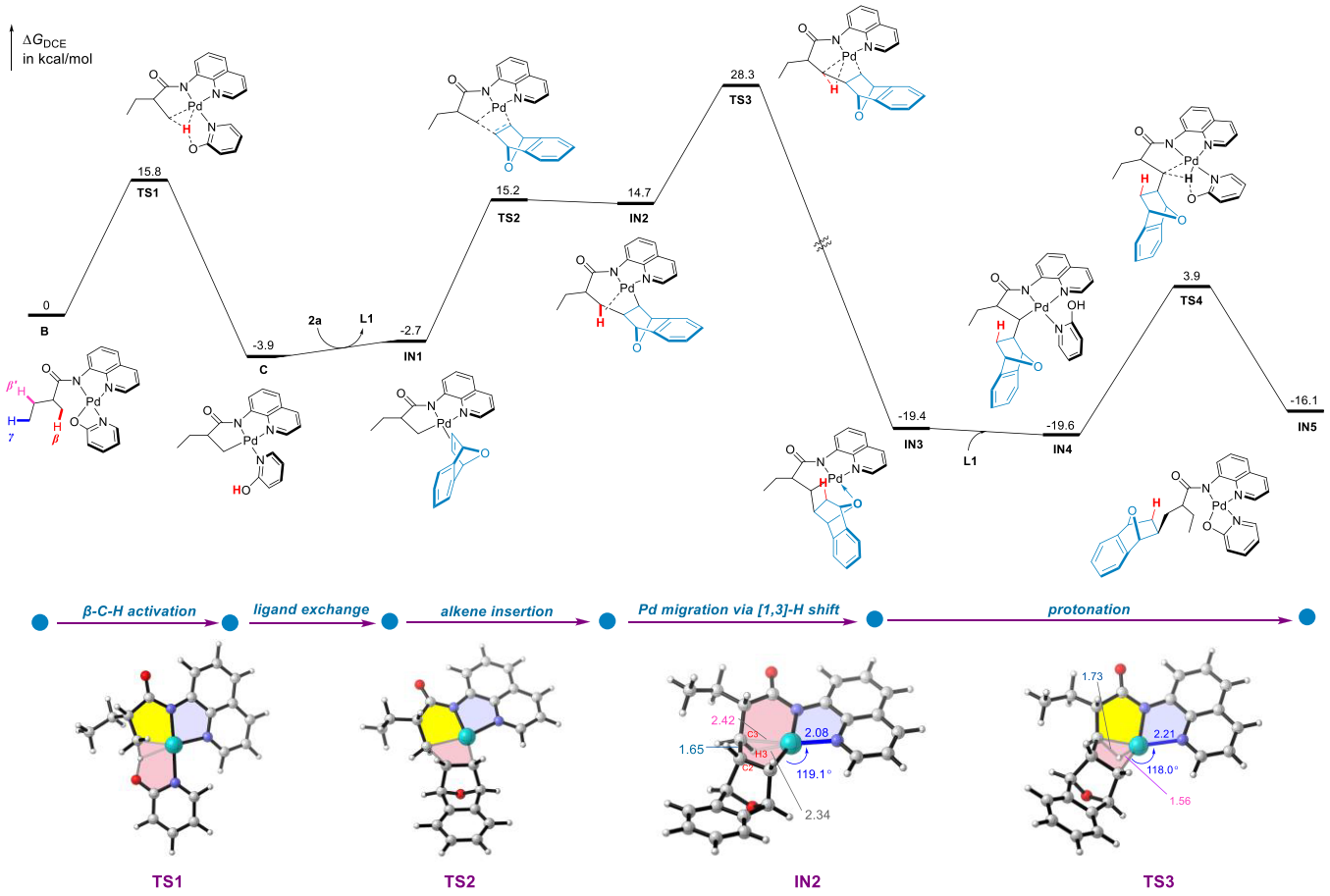

Figure 2. Gibbs energy profile of the β-alkylation pathway and molecular structures. Bond lengths are reported in Å. Computed at the SMD(DCE)/M06/def2-TZVPP//B3LYP/6-31G(d)/LANL2DZ level.

pathway, where the regiochemistry issue will also be discussed in detail.

Because Pd migration in the β pathway is difficult, this pathway has to make way for the γ pathway, which has an easier Pd migration process, on the basis of the Curtin−Hammett principle. In Figure 3, we present the β and γ pathways together, with more details of the stuctures of intermediates and transition states in the γ pathway. Let us discuss γ pathway and at the same time compare the γ and β pathways.

As expected, the γ pathway's C−H activation requires 20.8 kcal/mol, which is 5.0 kcal/mol higher than the 15.8 kcal/mol required in the β pathway. It has been well-documented that the formation of a six-membered palladacycle is kinetically less favored than the formation of a five-membered palladacycle,[35,63] which is consistent with our H/D exchange experiment (see the SI). Ligand exchange between **L1** and alkene **2a** gives **IN6**, which then undergoes alkene insertion to afford **IN7** which requires 11.9 kcal/mol (from **IN6** to **TS6**). This step is an exergonic process because of the formation of a larger ring, compared with the endergonic alkene insertion in β pathway (17.4 kcal/mol from **IN1** to **IN2**). The subsequent Pd migration requires 15.5 kcal/mol (from **IN7** to **TS7**), which is 1.9 kcal/mol higher than the similar process in the β pathway (13.6 kcal/mol, from **IN2** to **TS3**). From here we can immediately notice that the difficult Pd migration in the β pathway is due to the alkene insertion, which is thermodynamically disfavored and makes **TS3** become disfavored compared with **TS7** by 9.7 kcal/mol. Here we want to point out that direct protonation of **IN7** (similar to the direct protonation process in the β pathway) has an activation free energy of 34.9 kcal/mol (from **IN16** to **TS13** in Scheme 2), which also cannot occur under the experimental conditions.

According to the Curtin−Hammett principle, the reaction first undergoes β-C−H activation, followed by ligand exchange (easy) and alkene insertion (endergonic) to form intermediate **IN2**. Then the Pd migration is difficult, and the reaction has to go back to the starting material, which then undergoes γ-C−H activation, ligand exchange, alkene insertion (exergonic process) and Pd migration. The subsequent protonation to afford **IN11** is the turnover-limiting step, which requires 26.8 kcal/mol (from **IN9** to **TS10** in Figure 4). Then it is very easy for **IN11** to be transformed to the final product **3aa** (see SI).

Therefore, our calculations indicate that Pd migration instead of C−H activation has become the selectivity-determining step. Pd migration in the γ pathway is much favored compared with the β pathway, which leads to the selectivity.

Before we conclude this part, some details should be mentioned. To know why Pd migration plays such an important role in the γ selectivity, we also performed a careful analysis of the intermediates and transition states. As shown in Figure 2, the Pd−H3 distance in **IN2** is 2.34 Å, which means that there is a weak C−H→Pd agostic bond in **IN2**. This can be understood by **IN2**'s tricoordinate structure, which needs a C−H→Pd agostic bond[64] to make it more stable. In contrast **IN7** is much more stable than **IN2** because of the stronger C−H→Pd agostic bond: the Pd−H4 distance is only 1.92 Å, which is much shorter than

https://dx.doi.org/10.1021/acscatal.0c02025
ACS Catal. 2020, 10, 8212−8222

Scheme 2. Possible Direct Protonation Pathway for IN2 and IN7[a]

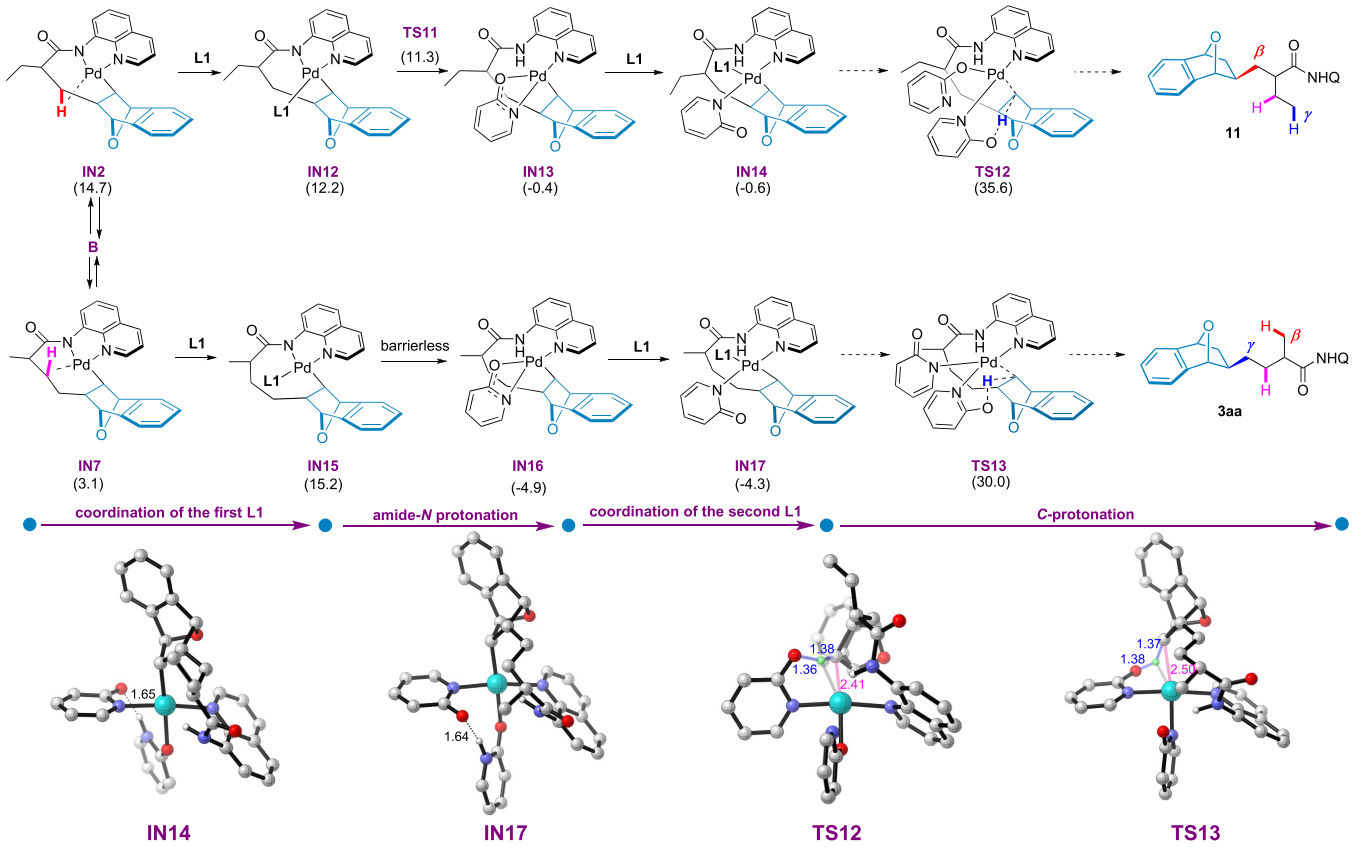

[a]Computed at the SMD(DCE)/M06/def2-TZVPP//B3LYP/6-31G(d)/LANL2DZ level and reported in kcal/mol. Some hydrogens have been omitted for clarity in the 3D molecular structures. Bond lengths are reported in Å.

the Pd−H3 distance in **IN2**, indicating that there is a strong C−H→Pd agostic interaction in **IN7**. There are two possible Pd migration pathways for γ-alkylation: 1,4-Pd migration via **TS7** and 1,3-Pd migration via **TS8**. However, there is only 1,3-Pd migration for β-alkylation. Intrinsic reaction coordinate (IRC) calculations indicated that the 1,3-Pd migration is a one-step process via a Pd(IV) transition state with a short Pd−H bond. It goes through a one-step oxidative hydrogen migration mechanism, which has been discussed in detail by Mota and Dedieu.[65,66] In contrast to the 1,3-Pd migration, the 1,4-Pd migration is found to occur in a stepwise manner involving an oxidative addition and reductive elimination mechanism. In the γ pathway, although 1,4-Pd migration is more favored, 1,3-Pd migration still cannot be ruled out because the energy difference is not big (1.3 kcal/mol). We attribute this energy difference to the more strained transition state structure of **TS8**. Compared with the β pathway, Pd migration in the γ pathway is favored for the following reasons. First, it can be seen in the structure of **IN7** (Figure 3) that the Pd−H4 distance is only 1.92 Å, which is much shorter than the Pd−H3 distance in **IN2** (2.34 Å) (Figure 2). This means H4 of **IN7** would be transferred more easily. Second, 1,4-Pd migration has a 5/5 ring transition state structure (**TS7**; see Figure 3), whereas the 1,3-Pd migration in the β pathway has a highly strained 5/4 ring transition state structure (**TS3**), which is less stable than a 5/5 ring transition state. Consequently, it would be much easier for the 1,4-Pd migration in the γ pathway to take place.

Why It Is Difficult for a General Alkene to React Under the Current Conditions. Here we discuss why a general alkene could not react under the current conditions so that we can understand why the present strategy of changing the C−H activation reaction can be applicable only to strained alkenes as used here (Scheme 3). Ethene was chosen as a model substate, and we found that the alkene insertion step for both the β pathway (from **IN18** to **TS14**, with an activation free energy of 30.0 kcal/mol) and the γ pathway (from **IN21** to **TS16**, with an activation free energy of 25.4 kcal/mol) is much more difficult than with strained bicyclic alkene **2a**. We also found that the Pd migration steps are very difficult, suggesting that general alkenes are not good candidates for the present reaction. Besides, the β-H elimination in each pathway is much more favored compared with Pd migration (see the SI for details), suggesting that these reactions may give undesired side products at elevated temperatures. Experimentally, when we treated 1-octene as the alkene substate under the standard conditions (Scheme 3), we found that the reactant was recovered in 93% yield and the desired reaction did not occur.

Experimental Support for the Reaction Mechanism. With the above mechanistic prediction that Pd migration is involved in the catalytic cycle, we carried out experiments to get evidence to support our mechanism at the same time. Several key intermediates were synthesized and characterized by us. The five-membered palladacycle **Int-A** obtained from isobutyramide bearing no γ-C(sp^3)−H bonds failed to deliver the alkylation product under the standard conditions (Scheme 4a), which is consistent with our DFT calculations. The reaction of 2-methylbutanamide **1a** bearing both β- and γ-methyl C−H bonds with $Pd(OAc)_2$ afforded the five-membered palladacycle **Int-B**

https://dx.doi.org/10.1021/acscatal.0c02025
ACS Catal. 2020, 10, 8212−8222

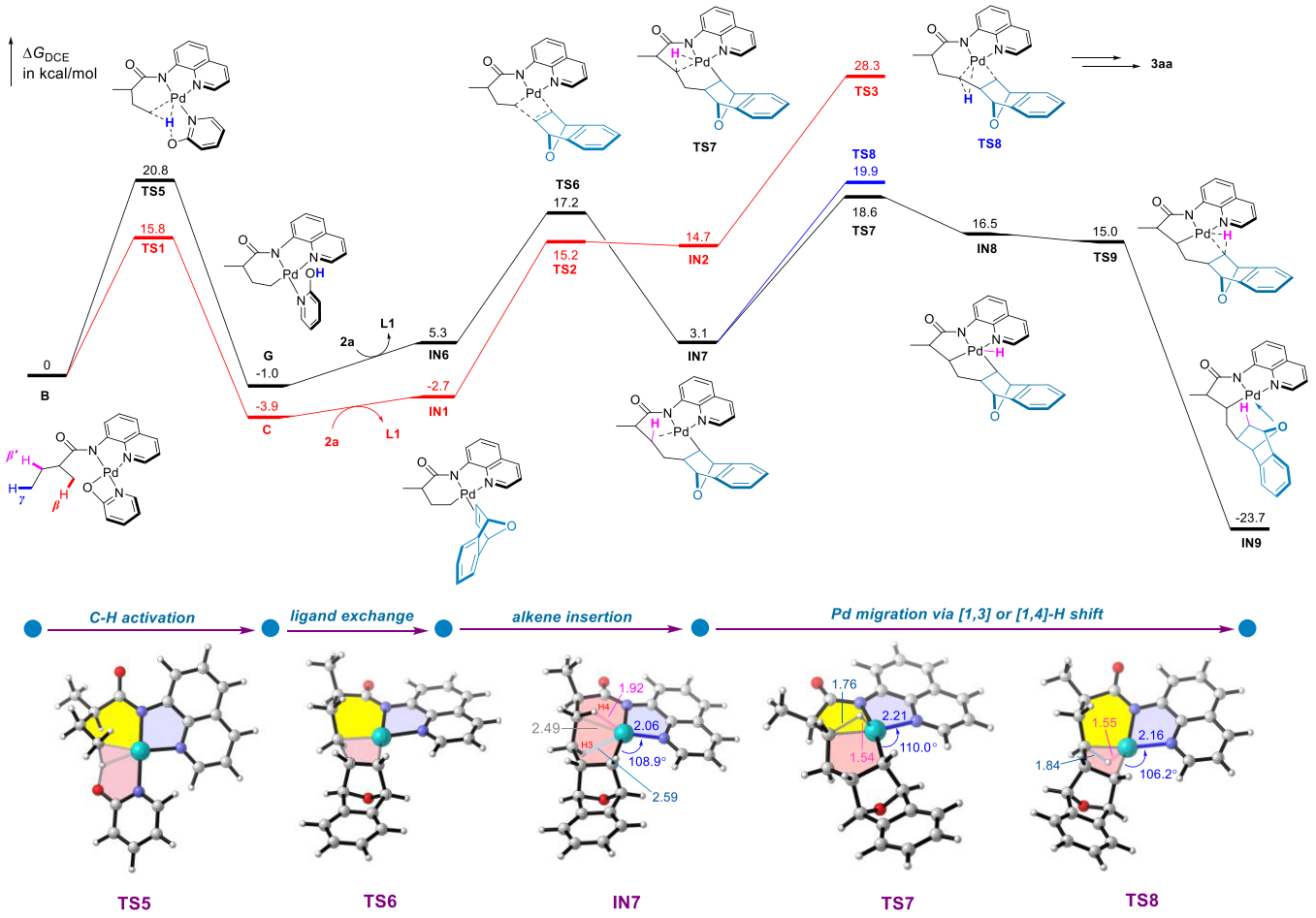

Figure 3. Gibbs energy profiles for the γ-alkylation pathway and the β-alkylation pathway along with molecular structures. Bond lengths are reported in Å. Computed at the SMD(DCE)/M06/def2-TZVPP//B3LYP/6-31G(d)/LANL2DZ level.

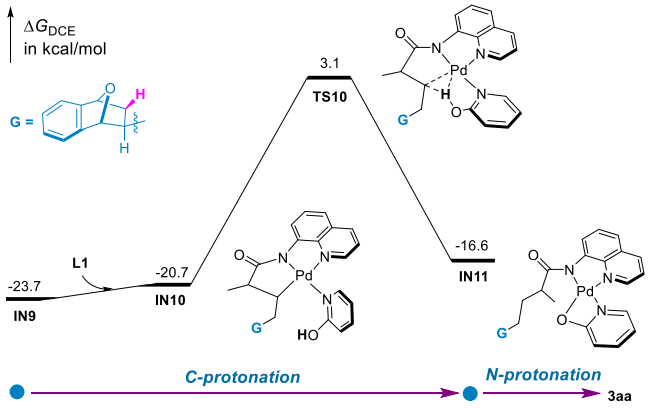

Figure 4. Gibbs energy profile for the protonation process in the γ-alkylation pathway. Computed at the SMD(DCE)/M06/def2-TZVPP//B3LYP/6-31G(d)/LANL2DZ level.

through β-methyl C−H activation in 93% yield in 30 min, while all attempts to obtain the corresponding six-membered palladacycle through γ-C−H activation from **1a** were unsuccessful.

Fortunately, the six-membered palladacycle **Int-C** was successfully synthesized from 3,3-dimethylbutanamide and unambiguously confirmed by X-ray crystallography. Stoichiometric reactions of **Int-B** and **Int-C** were then conducted. The reaction of **Int-B** failed to afford the β-alkylated product and

Scheme 3. γ-C(sp^3)−H Functionalization with General Alkene and Calculated Pathway with Ethene as the Model Substrate[a]

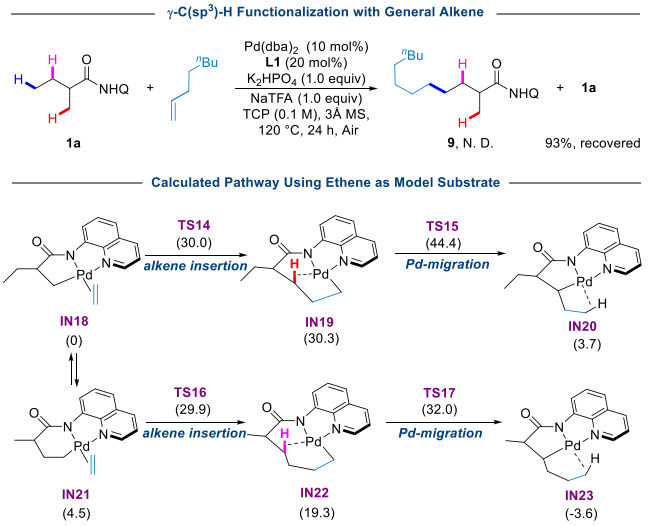

[a]Computed at the SMD(DCE)/M06/def2-TZVPP//B3LYP/6-31G(d)/LANL2DZ level and reported in kcal/mol.

solely gave the γ-alkylated product **3aa** in 52% yield (Scheme 4b). **Int-C** reacted smoothly to give the γ-alkylated product **3ka**

https://dx.doi.org/10.1021/acscatal.0c02025
ACS Catal. 2020, 10, 8212−8222

Scheme 4. Experimental Mechanistic Studies by Synthesis, Characterization, and Reaction of Various Palladacycles

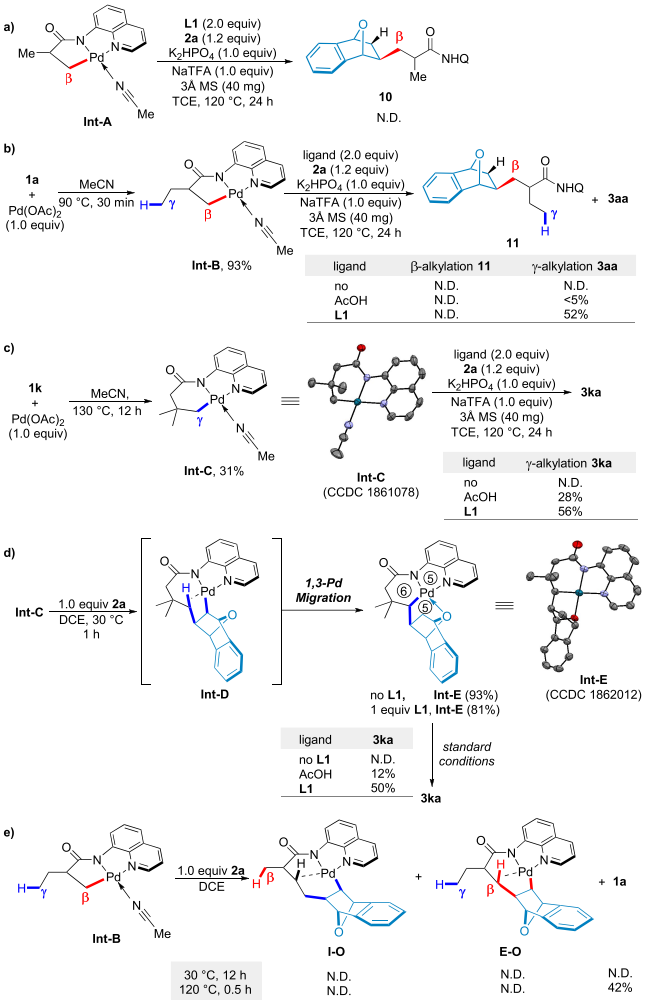

in 56% yield, as expected (Scheme 4c). As shown in Scheme 4b,c, 2-pyridone (**L1**) is crucial for the reaction of those palladacycles, as no product was observed in the absence of **L1**. We envisioned that this might provide a unique opportunity to prepare the alkene insertion intermediates. A mixture of **Int-C** with **2a** was then stirred in DCE at 30 °C (Scheme 4d). After 1 h, a bright-yellow precipitate, **Int-E**, was observed and obtained in 93% yield. Notably, in a parallel experiment in the presence of **L1**, **Int-E** was also generated exclusively. These results suggested that **L1** might not be invovled in the migratory insertion step (Figure 1, **I** → **J**). The structure of **Int-E** was unambiguously assigned as an usual [5,6,5] fused palladacycle, which might be formed by 1,3-Pd migration from the migratory insertion intermediate, palladacycle **Int-D**.[67−69] This is highly consistent with our DFT predictions. The reaction of **Int-B** with **2a** was also performed, but no migratory insertion intermediates or related intermediates were detected even at an elevated temperature (Scheme 4e). Therefore, we can also conclude that the Pd migration step is the key determinant for γ-selectivity experimentally.

We also observed that **L1** was crucial for the final protonation step (Scheme 4d, **Int-E** → **3ka**), which was explained in detail by computations (Figure S10). Ligand **L1** was also an efficient promoter of the γ-C−H cyclopalladation, as the H/D exchange experiments (see the SI) and DFT studies (Figure S2) showed that ligand **L1** leads to slightly better deuteration incorporation and a lower energy barrier than the carboxylic acids.

Actually, most Pd migration occurs in an acyclic manner,[62] and intraring Pd migration like this has scarcely been reported, to the best of our knowledge. Besides, this is the first example of a C(sp^3) to C(sp^3) Pd migration process. In order to further confirm that the unique Pd migration step indeed occurred in our reactions, we did a deuterium labeling experiment (Scheme 5). Substrate **1k** was chosen to be labeled because it can only

Scheme 5. Deuterium Labeling Experiments

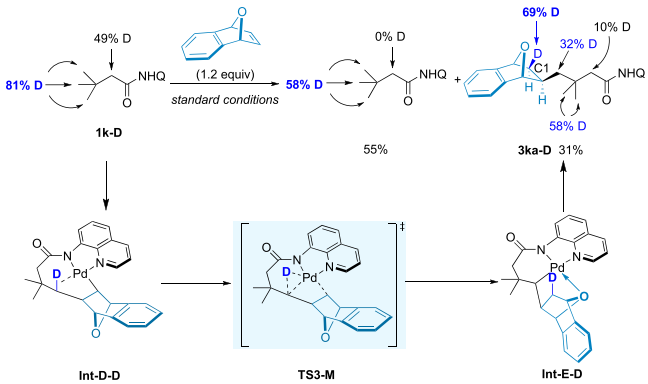

undergo 1,3-Pd migration, which would be easier to observe without being affected by 1,4-Pd migration. After obtaining **1k-D** with 81% deuterium labeling on its methyl hydrogens, we did the reaction using **1k-D** as the substrate under the standard conditions. As expected, deuterium-labeled product **3ka-D** was indeed isolated in 31% yield with 55% recovery of **1k-D**. The product with deuterium labeled on C1 should come from 1,3-Pd migration of **Int-D-D** via **TS3-M**. The deuterium labeling ratio of C1 of **3ka-D** is a little smaller than that of **1k-D**, which can be explained by the kinetic isotope effect that H atoms are transferred faster than D atoms. With this convincing experiment and DFT calculation result combined with the X-ray structure of **Int-E**, we can conclude that the Pd migration step is involved the catalytic cycle.

CONCLUSION

We have disclosed a ligand-enabled Pd-catalyzed site-selective γ-C(sp^3)−H alkylation of aliphatic carboxamides with strained bicyclic alkenes using a new strategy (strategy II). This strategy was realized by changing the regiodetermining step from the common C−H activation step to an unexpected Pd migration step. This catalytic method overcomes the long-held drawback that C−H bond functionalization occurs at the β-position via the kinetically more favorable five-membered C−H cyclopalladation. In our case, C−H activation and alkene insertion in the β pathway are still favored over the γ pathway. After that, however, in contrast to previous reports, direct protonation of both pathways is disfavored. Instead, an unexpected Pd migration process occurs, which favors the γ pathway and leads to the γ selectivity. To the best of our knowledge, this is the first C(sp^3) to C(sp^3) Pd migration process. This mechanism was supported by DFT calculations, X-ray structures of some important palladacycle intermediates, stoichiometric experiments, and the deuterium labeling experiment. Sequential functionalization of the remaining β-C(sp^3)−H bond offers a practical approach to access multifunctionalized products from simple molecules. We anticipate that these insights will inspire the development of

https://dx.doi.org/10.1021/acscatal.0c02025
ACS Catal. 2020, 10, 8212−8222

unconventional site-selective remote C−H activation reactions of aliphatic molecules.

COMPUTATIONAL METHODS

DFT calculations with the Gaussian 09 program[70] were used to explore the mechanism of the reaction. The B3LYP functional[71,72] was used to optimize the geometries of all stationary points in the gas phase with the LANL2DZ basis set[73] for palladium and 6-31G(d) basis set[74] for the other atoms. The keyword "5D" was used to specify that five d-type orbitals were used for all elements in structure optimization. For each optimized structure, unscaled harmonic frequencies were computed to validated the structure as either an energy minimum or a transition state and to evaluate its zero-point energy and thermal corrections at 298 K. IRC calculations[75] were carried out to confirm that the key transition state structures connect corresponding reactants and products. Quasi-harmonic corrections were applied during the entropy calculations by setting all of the positive frequencies that were less than 100 cm^{-1} to 100 cm^{-1} using GoodVibes.[76,77] For the optimized structures, single-point energy calculations were performed at the SMD(DCE)/M06/def2-TZVPP level of theory.[78−80] 1,2-Dichloroethane (DCE), in which the reaction can also occur, was chosen as the solvent to replace 1,2,3-trichloropropane (TCP) for computing because TCP, which was used for the further scope investigation, was not defined in the SMD model of Gaussian 09. Pruned integration grids with 99 radial shells and 590 angular points per shell were used during single-point energy calculation. Reference states for gases and solutes in DCE solution are the hypothetical states at 1 atm and 1 mol/L, respectively. All of the graphics of molecular structures were prepared using CYLview.[81]

ASSOCIATED CONTENT

Supporting Information

The Supporting Information is available free of charge at https://pubs.acs.org/doi/10.1021/acscatal.0c02025.

Experimental procedures and spectral data for all new compounds (PDF)

Crystallographic data for **Int-C** (CIF)

Crystallographic data for **Int-E** (CIF)

AUTHOR INFORMATION

Corresponding Authors

Bing-Feng Shi − *Department of Chemistry, Zhejiang University, Hangzhou 310027, China;* orcid.org/0000-0003-0375-955X; Email: bfshi@zju.edu.cn

Zhi-Xiang Yu − *Beijing National Laboratory for Molecular Sciences (BNLMS), Key Laboratory of Bioorganic Chemistry and Molecular Engineering of Ministry of Education, College of Chemistry, Peking University, Beijing 100871, China;* orcid.org/0000-0003-0939-9727; Email: yuzx@pku.edu.cn

Authors

Ya Li − *Department of Chemistry, Zhejiang University, Hangzhou 310027, China*

Pan Zhang − *Beijing National Laboratory for Molecular Sciences (BNLMS), Key Laboratory of Bioorganic Chemistry and Molecular Engineering of Ministry of Education, College of Chemistry, Peking University, Beijing 100871, China*

Yue-Jin Liu − *Department of Chemistry, Zhejiang University, Hangzhou 310027, China*

Complete contact information is available at: https://pubs.acs.org/10.1021/acscatal.0c02025

Author Contributions

§Y.L. and P.Z. contributed equally.

Notes

The authors declare no competing financial interest.

The crystallographic data for **Int-C** (CCDC 1861078) and **Int-E** (CCDC 1862012) have also been deposited at the Cambridge Crystallographic Data Centre.

ACKNOWLEDGMENTS

Financial support from the National Natural Science Foundation of China (21925109, 21772170, and 21933003), the Outstanding Young Talents of Zhejiang Province High-Level Personnel of Special Support (ZJWR0108), the Zhejiang Provincial NSFC (LR17B020001), and the Fundamental Research Funds for the Central Universities (2018XZZX001-02) is gratefully acknowledged. We are also grateful for the computational resources provided by the High-Performance Computing Platform of Peking University and Prof. Ji-Yong Liu (Zhejiang University) for help with X-ray analysis. Dedicated to the 70th anniversary of Shanghai Institute of Organic Chemistry, CAS.

REFERENCES

(1) Daugulis, O.; Do, H.-Q.; Shabashov, D. Palladium- and Copper-Catalyzed Arylation of Carbon−Hydrogen Bonds. *Acc. Chem. Res.* **2009**, *42*, 1074.

(2) Jazzar, R.; Hitce, J.; Renaudat, A.; Sofack-Kreutzer, J.; Baudoin, O. Functionalization of Organic Molecules by Transition-Metal-Catalyzed C(sp^3)−H Activation. *Chem. - Eur. J.* **2010**, *16*, 2654.

(3) Lyons, T. W.; Sanford, M. S. Palladium-Catalyzed Ligand-Directed C−H Functionalization Reactions. *Chem. Rev.* **2010**, *110*, 1147.

(4) Newhouse, T.; Baran, P. S. If C−H Bonds Could Talk: Selective C−H Bond Oxidation. *Angew. Chem., Int. Ed.* **2011**, *50*, 3362.

(5) Baudoin, O. Transition metal-catalyzed arylation of unactivated C(sp^3)−H bonds. *Chem. Soc. Rev.* **2011**, *40*, 4902.

(6) Rouquet, G.; Chatani, N. Catalytic Functionalization of C(sp^2)−H and C(sp^3)−H Bonds by Using Bidentate Directing Groups. *Angew. Chem., Int. Ed.* **2013**, *52*, 11726.

(7) Daugulis, O.; Roane, J.; Tran, L. D. Bidentate, Monoanionic Auxiliary-Directed Functionalization of Carbon−Hydrogen Bonds. *Acc. Chem. Res.* **2015**, *48*, 1053.

(8) He, G.; Wang, B.; Nack, W. A.; Chen, G. Syntheses and Transformations of α-Amino Acids via Palladium-Catalyzed Auxiliary-Directed sp^3 C−H Functionalization. *Acc. Chem. Res.* **2016**, *49*, 635.

(9) Zhang, Q.; Shi, B.-F. From Reactivity and Regioselectivity to Stereoselectivity: An Odyssey of Designing PIP Amine and Related Directing Groups for C-H Activation. *Chin. J. Chem.* **2019**, *37*, 647.

(10) He, J.; Wasa, M.; Chan, K. S. L.; Shao, Q.; Yu, J.-Q. Palladium-Catalyzed Transformations of Alkyl C−H Bonds. *Chem. Rev.* **2017**, *117*, 8754.

(11) Xu, Y.; Dong, G. sp^3 C−H activation via *exo*-type directing groups. *Chem. Sci.* **2018**, *9*, 1424.

(12) Chu, J. C. K.; Rovis, T. Complementary Strategies for Directed C(sp^3)−H Functionalization: A Comparison of Transition-Metal-Catalyzed Activation, Hydrogen Atom Transfer, and Carbene/Nitrene Transfer. *Angew. Chem., Int. Ed.* **2018**, *57*, 62.

(13) Chen, Z.; Rong, M.-Y.; Nie, J.; Zhu, X.-F.; Shi, B.-F.; Ma, J.-A. Catalytic Alkylation of Unactivated C(sp3)-H Bonds for C(sp^3)-C(sp^3) Bond Formation. *Chem. Soc. Rev.* **2019**, *48*, 4921.

(14) Hartwig, J. F. Regioselectivity of the borylation of alkanes and arenes. *Chem. Soc. Rev.* **2011**, *40*, 1992.

(15) Huang, Z.; Dong, G. Site-Selectivity Control in Organic Reactions: A Quest to Differentiate Reactivity among the Same Kind of Functional Groups. *Acc. Chem. Res.* **2017**, *50*, 465.
(16) Ping, L.; Chung, D. S.; Bouffard, J.; Lee, S.-G. Transition metal-catalyzed site- and regio-divergent C−H bond functionalization. *Chem. Soc. Rev.* **2017**, *46*, 4299.
(17) Hartwig, J. F. Catalyst-Controlled Site-Selective Bond Activation. *Acc. Chem. Res.* **2017**, *50*, 549.
(18) Sambiagio, C.; Schönbauer, D.; Blieck, R.; Dao-Huy, T.; Pototschnig, G.; Schaaf, P.; Wiesinger, T.; Zia, M. F.; Wencel-Delord, J.; Besset, T.; Maes, B. U. W.; Schnürch, M. A comprehensive overview of directing groups applied in metal-catalyzed C−H functionalization chemistry. *Chem. Soc. Rev.* **2018**, *47*, 6603−6743.
(19) Reddy, B. V. S.; Reddy, L. R.; Corey, E. J. Novel Acetoxylation and C−C Coupling Reactions at Unactivated Positions in α-Amino Acid Derivatives. *Org. Lett.* **2006**, *8*, 3391.
(20) Ano, Y.; Tobisu, M.; Chatani, N. Palladium-Catalyzed Direct Ethynylation of C(sp^3)−H Bonds in Aliphatic Carboxylic Acid Derivatives. *J. Am. Chem. Soc.* **2011**, *133*, 12984.
(21) He, G.; Zhang, S.-Y.; Nack, W. A.; Li, Q.; Chen, G. Use of a Readily Removable Auxiliary Group for the Synthesis of Pyrrolidones by the Palladium-Catalyzed Intramolecular Amination of Unactivated γ C(sp^3) − H Bonds. *Angew. Chem., Int. Ed.* **2013**, *52*, 11124.
(22) He, G.; Zhang, S.-Y.; Nack, W. A.; Pearson, R.; Rabb-Lynch, J.; Chen, G. Total Synthesis of Hibispeptin A via Pd-Catalyzed C(sp^3)−H Arylation with Sterically Hindered Aryl Iodides. *Org. Lett.* **2014**, *16*, 6488.
(23) Chen, K.; Hu, F.; Zhang, S.-Q.; Shi, B.-F. Pd(II)-catalyzed alkylation of unactivated C(sp^3)−H bonds: efficient synthesis of optically active unnatural α-amino acids. *Chem. Sci.* **2013**, *4*, 3906.
(24) Dey, A.; Pimparkar, S.; Deb, A.; Guin, S.; Maiti, D. Chelation-Assisted PalladiumCatalyzed γ-Arylation of Aliphatic Carboxylic Acid Derivatives. *Adv. Synth. Catal.* **2017**, *359*, 1301.
(25) Thrimurtulu, N.; Khan, S.; Maity, S.; Volla, C. M. R.; Maiti, D. Palladium catalyzed direct aliphatic γ-C(sp3)−H alkenylation with alkenes and alkenyl iodides. *Chem. Commun.* **2017**, *53*, 12457.
(26) Deb, A.; Singh, S. S.; Seth, K.; Pimparkar, S.; Bhaskararao, B.; Guin, S.; Sunoj, R. B.; Maiti, D. Experimental and Computational Studies on Remote γ-C(sp3)−H Silylation and Germanylation of Aliphatic Carboxamides. *ACS Catal.* **2017**, *7*, 8171.
(27) Guin, S.; Deb, A.; Dolui, P.; Chakraborty, S.; Singh, V. K.; Maiti, D. Promoting Highly Diastereoselective γ-C−H Chalcogenation of α-Amino Acids and Aliphatic Carboxylic Acids. *ACS Catal.* **2018**, *8*, 2664.
(28) Zaitsev, V. G.; Shabashov, D.; Daugulis, O. Highly Regioselective Arylation of sp^3 C−H Bonds Catalyzed by Palladium Acetate. *J. Am. Chem. Soc.* **2005**, *127*, 13154.
(29) Li, S.; Chen, G.; Feng, C.-G.; Gong, W.; Yu, J.-Q. Ligand-Enabled γ-C−H Olefination and Carbonylation: Construction of β-Quaternary Carbon Centers. *J. Am. Chem. Soc.* **2014**, *136*, 5267.
(30) Li, S.; Zhu, R.-Y.; Xiao, K.-J.; Yu, J.-Q. Ligand-Enabled Arylation of γ-C−H Bonds. *Angew. Chem., Int. Ed.* **2016**, *55*, 4317.
(31) Dolui, P.; Das, J.; Chandrashekar, H. B.; Anjana, S. S.; Maiti, D. Ligand-Enabled Pd^{II}-Catalyzed Iterative γ-C(sp^3)−H Arylation of Free Aliphatic Acid. *Angew. Chem., Int. Ed.* **2019**, *58*, 13773−13777.
(32) Liu, L.; Liu, Y.-H.; Shi, B.-F. Synthesis of Amino Acids and Peptides with Bulky Side Chains via Ligand-Enabled Carboxylate-Directed γ-C(sp^3)−H Arylation. *Chem. Sci.* **2020**, *11*, 290−294.
(33) Chen, Y.-Q.; Wang, Z.; Wu, Y.-W.; Wisniewski, S. R.; Qiao, J. X.; Ewing, W. R.; Eastgate, M. D.; Yu, J.-Q. Overcoming the Limitations of gamma, and delta-C−H Arylation of Amines through Ligand Development. *J. Am. Chem. Soc.* **2018**, *140*, 17884−17894.
(34) Xia, G.-Q.; Weng, J.; Liu, L.-Y.; Verma, P.; Li, Z.-Q.; Yu, J.-Q. Reversing conventional site-selectivity in C(sp^3)−H bond activation. *Nat. Chem.* **2019**, *11*, 571−577.
(35) Xu, J.-W.; Zhang, Z.-Z.; Rao, W.-H.; Shi, B.-F. Site-Selective Alkenylation of δ-C(sp^3)−H Bonds with Alkynes via a Six-Membered Palladacycle. *J. Am. Chem. Soc.* **2016**, *138*, 10750.
(36) Zhan, B.-B.; Li, Y.; Xu, J.-W.; Nie, X.-L.; Fan, J.; Jin, L.; Shi, B.-F. Site-Selective δ-C(sp^3)−H Alkylation of Amino Acids and Peptides with Maleimides via a Six-Membered Palladacycle. *Angew. Chem., Int. Ed.* **2018**, *57*, 5858.
(37) Seeman, J. I. Effect of conformational change on reactivity in organic chemistry. Evaluations, applications, and extensions of Curtin−Hammett Winstein−Holness kinetics. *Chem. Rev.* **1983**, *83*, 83−134.
(38) Chen, D.-F.; Chu, J. C. K.; Rovis, T. Directed γ-C(sp^3)−H Alkylation of Carboxylic Acid Derivatives through Visible Light Photoredox Catalysis. *J. Am. Chem. Soc.* **2017**, *139*, 14897.
(39) Wang, F.; Yu, S.; Li, X. Transition metal-catalysed couplings between arenes and strained or reactive rings: combination of C−H activation and ring scission. *Chem. Soc. Rev.* **2016**, *45*, 6462.
(40) Qi, Z.-S.; Li, X. Rhodium(III)-Catalyzed Coupling of Arenes with 7-Oxa/Azabenzonorbornadienes by C−H Activation. *Angew. Chem., Int. Ed.* **2013**, *52*, 8995−9000.
(41) Dong, W.-R.; Parthasarathy, K.; Cheng, Y.; Pan, F.-F.; Bolm, C. Hydroarylations of Heterobicyclic Alkenes through Rhodium-Catalyzed Directed C−H Functionalizations of S-Aryl Sulfoximines. *Chem. - Eur. J.* **2014**, *20*, 15732.
(42) Gandeepan, P.; Rajamalli, P.; Cheng, C.-H. Diastereoselective [3 + 2] Annulation of Aromatic/Vinylic Amides with Bicyclic Alkenes through Cobalt-Catalyzed C−H Activation and Intramolecular Nucleophilic Addition. *Angew. Chem., Int. Ed.* **2016**, *55*, 4308.
(43) Wang, X.-M.; Lerchen, A.; Gensch, T.; Knecht, T.; Daniliuc, C. G.; Glorius, F. Combination of Cp*Rh^{III}-Catalyzed C−H Activation and a Wagner−Meerwein-Type Rearrangement. *Angew. Chem., Int. Ed.* **2017**, *56*, 1381.
(44) Wang, P.; Farmer, M. E.; Huo, X.; Jain, P.; Shen, P.-X.; Ishoey, M.; Bradner, J. E.; Wisniewski, S. R.; Eastgate, M. D.; Yu, J.-Q. Ligand-Promoted *Meta*-C−H Arylation of Anilines, Phenols, and Heterocycles. *J. Am. Chem. Soc.* **2016**, *138*, 9269.
(45) Wang, P.; Li, G.-C.; Jain, P.; Farmer, M. E.; He, J.; Shen, P.-X.; Yu, J.-Q. Ligand-Promoted *meta*-C−H Amination and Alkynylation. *J. Am. Chem. Soc.* **2016**, *138*, 14092.
(46) Wang, P.; Farmer, M. E.; Yu, J.-Q. Ligand-Promoted *meta*-C−H Functionalization of Benzylamines. *Angew. Chem., Int. Ed.* **2017**, *56*, 5125.
(47) Li, G.-C.; Wang, P.; Farmer, M. E.; Yu, J.-Q. Ligand-Enabled Auxiliary-Free *meta*-C−H Arylation of Phenylacetic Acids. *Angew. Chem., Int. Ed.* **2017**, *56*, 6874.
(48) Wang, P.; Verma, P.; Xia, G.-Q.; Shi, J.; Qiao, J. X.; Tao, S.-W.; Cheng, P. T. W.; Poss, M. A.; Farmer, M. E.; Yeung, K.-S.; Yu, J.-Q. Ligand-accelerated non-directed C−H functionalization of arenes. *Nature* **2017**, *551*, 489.
(49) Zhu, R.-Y.; Li, Z.-Q.; Park, H. S.; Senanayake, C. H.; Yu, J.-Q. Ligand-Enabled γ-C(sp^3)−H Activation of Ketones. *J. Am. Chem. Soc.* **2018**, *140*, 3564.
(50) Wang, D.; Weinstein, A. B.; White, P. B.; Stahl, S. S. Ligand-Promoted Palladium-Catalyzed Aerobic Oxidation Reactions. *Chem. Rev.* **2018**, *118*, 2636.
(51) Gligorich, K. M.; Sigman, M. S. Mechanistic Questions about the Reaction of Molecular Oxygen with Palladium in Oxidase Catalysis. *Angew. Chem., Int. Ed.* **2006**, *45*, 6612.
(52) Dai, H.-X.; Yu, J.-Q. Pd-Catalyzed Oxidative *ortho*-C−H Borylation of Arenes. *J. Am. Chem. Soc.* **2012**, *134*, 134.
(53) Mao, J.; Zhang, S.-Q.; Shi, B.-F.; Bao, W. Palladium(0)-Catalyzed Cyclopropanation of Benzyl Bromides via C(sp^3)−H Bond Activation. *Chem. Commun.* **2014**, *50*, 3692.
(54) Lautens, M.; Fagnou, K.; Hiebert, S. Transition Metal-Catalyzed Enantioselective Ring-Opening Reactions of Oxabicyclic Alkenes. *Acc. Chem. Res.* **2003**, *36* (1), 48−58.
(55) Liu, Y.-J.; Liu, Y.-H.; Zhang, Z.-Z.; Yan, S.-Y.; Chen, K.; Shi, B.-F. Divergent and Stereoselective Synthesis of β-Silyl-α-Amino Acids through Palladium-Catalyzed Intermolecular Silylation of Unactivated Primary and Secondary C−H Bonds. *Angew. Chem., Int. Ed.* **2016**, *55*, 13859.
(56) Liao, G.; Yin, X.-S.; Chen, K.; Zhang, Q.; Zhang, S.-Q.; Shi, B.-F. Stereoselective alkoxycarbonylation of unactivated C(sp^3)−H bonds with alkyl chloroformates via Pd(II)/Pd(IV) catalysis. *Nat. Commun.* **2016**, *7*, 12901.

https://dx.doi.org/10.1021/acscatal.0c02025
ACS Catal. 2020, 10, 8212−8222

(57) Zhang, S.-Y.; Li, Q.; He, G.; Nack, W. A.; Chen, G. Stereoselective Synthesis of β-Alkylated α-Amino Acids via Palladium-Catalyzed Alkylation of Unactivated Methylene C(sp^3)−H Bonds with Primary Alkyl Halides. *J. Am. Chem. Soc.* **2013**, *135*, 12135.
(58) Wang, B.; Lu, C.-X.; Zhang, S.-Y.; He, G.; Nack, W. A.; Chen, G. Palladium-Catalyzed Stereoretentive Olefination of Unactivated C(sp3)−H Bonds with Vinyl Iodides at Room Temperature: Synthesis of β-Vinyl α-Amino Acids. *Org. Lett.* **2014**, *16*, 6260.
(59) Chen, K.; Zhang, S.-Q.; Xu, J.-W.; Hu, F.; Shi, B.-F. A general and practical palladium-catalyzed monoarylation of β-methyl C(sp^3)−H of alanine. *Chem. Commun.* **2014**, *50*, 13924.
(60) Gorelsky, S. I.; Lapointe, D.; Fagnou, K. Analysis of the Concerted Metalation-Deprotonation Mechanism in Palladium-Catalyzed Direct Arylation Across a Broad Range of Aromatic Substrates. *J. Am. Chem. Soc.* **2008**, *130*, 10848.
(61) Xing, Y.-Y.; Liu, J.-B.; Sun, C.-Z.; Huang, F.; Chen, D.-Z. The underlying factors controlling the Pd-catalyzed site-selective alkenylation of aliphatic amines. *Dalton Trans.* **2017**, *46*, 9430.
(62) Rahim, A.; Feng, J.; Gu, Z. 1,4-Migration of Transition Metals in Organic Synthesis. *Chin. J. Chem.* **2019**, *37*, 929.
(63) He, G.; Zhao, Y.-S.; Zhang, S.-Y.; Lu, C.-X.; Chen, G. Highly Efficient Syntheses of Azetidines, Pyrrolidines, and Indolines via Palladium Catalyzed Intramolecular Amination of C(sp^3)−H and C(sp^2)−H Bonds at γ and δ Positions. *J. Am. Chem. Soc.* **2012**, *134*, 3−6.
(64) Brookhart, M.; Green, M. L. H.; Parkin, G. Agostic interactions in transition metal compounds. *Proc. Natl. Acad. Sci. U. S. A.* **2007**, *104*, 6908.
(65) Mota, A. J.; Dedieu, A. Intramolecular 1,n Palladium Migrations in Polycyclic Aromatic Hydrocarbons. Palladium(II) versus Palladium(IV) Mechanisms: A Theoretical Study. *Organometallics* **2006**, *25*, 3130.
(66) Mota, A. J.; Dedieu, A. Through-Space Intramolecular Palladium Rearrangement in Substituted Aryl Complexes: Theoretical Study of the Aryl to Alkylpalladium Migration Process. *J. Org. Chem.* **2007**, *72*, 9669.
(67) Ma, S.-M.; Gu, Z.-H. 1,4-Migration of Rhodium and Palladium in Catalytic Organometallic Reactions. *Angew. Chem., Int. Ed.* **2005**, *44*, 7512.
(68) Shi, F.; Larock, R. C. Remote C−H activation via through-space palladium and rhodium migrations. *Top. Curr. Chem.* **2009**, *292*, 123.
(69) Zhang, J.; Liu, J.-F.; Ugrinov, A.; Pillai, A. F. X.; Sun, Z.-M.; Zhao, P. Methoxy-Directed Aryl-to-Aryl 1,3-Rhodium Migration. *J. Am. Chem. Soc.* **2013**, *135*, 17270.
(70) Frisch, M. J.; Trucks, G. W.; Schlegel, H. B.; Scuseria, G. E.; Robb, M. A.; Cheeseman, J. R.; Scalmani, G.; Barone, V.; Mennucci, B.; Petersson, G. A.; Nakatsuji, H.; Caricato, M.; Li, X.; Hratchian, H. P.; Izmaylov, A. F.; Bloino, J.; Zheng, G.; Sonnenberg, J. L.; Hada, M.; Ehara, M.; Toyota, K.; Fukuda, R.; Hasegawa, J.; Ishida, M.; Nakajima, T.; Honda, Y.; Kitao, O.; Nakai, H.; Vreven, T.; Montgomery, J. A., Jr.; Peralta, J. E.; Ogliaro, F.; Bearpark, M.; Heyd, J. J.; Brothers, E.; Kudin, K. N.; Staroverov, V. N.; Kobayashi, R.; Normand, J.; Raghavachari, K.; Rendell, A.; Burant, J. C.; Iyengar, S. S.; Tomasi, J.; Cossi, M.; Rega, N.; Millam, J. M.; Klene, M.; Knox, J. E.; Cross, J. B.; Bakken, V.; Adamo, C.; Jaramillo, J.; Gomperts, R.; Stratmann, R. E.; Yazyev, O.; Austin, A. J.; Cammi, R.; Pomelli, C.; Ochterski, J. W.; Martin, R. L.; Morokuma, K.; Zakrzewski, V. G.; Voth, G. A.; Salvador, P.; Dannenberg, J. J.; Dapprich, S.; Daniels, A. D.; Farkas, Ö.; Foresman, J. B.; Ortiz, J. V.; Cioslowski, J.; Fox, D. J. *Gaussian 09*, rev. E.01; Gaussian, Inc.: Wallingford, CT, 2013.
(71) Becke, A. D. Density-functional thermochemistry. III. The role of exact exchange. *J. Chem. Phys.* **1993**, *98*, 5648.
(72) Lee, C.; Yang, W.; Parr, R. G. Development of the Colle-Salvetti correlation-energy formula into a functional of the electron density. *Phys. Rev. B: Condens. Matter Mater. Phys.* **1988**, *37*, 785.
(73) Hay, P. J.; Wadt, W. R. *Ab initio* effective core potentials for molecular calculations. Potentials for the transition metal atoms Sc to Hg. *J. Chem. Phys.* **1985**, *82*, 270.
(74) Hehre, W. J.; Radom, L.; Schleyer, P. v. R.; Pople, J. A. *Ab Initio Molecular Orbital Theory*; Wiley: New York, 1986.
(75) Fukui, K. Formulation of the reaction coordinate. *J. Phys. Chem.* **1970**, *74*, 4161.
(76) Ribeiro, R. F.; Marenich, A. V.; Cramer, C. J.; Truhlar, D. G. Use of Solution-Phase Vibrational Frequencies in Continuum Models for the Free Energy of Solvation. *J. Phys. Chem. B* **2011**, *115*, 14556.
(77) Luchini, G.; Alegre-Requena, J. V.; Funes-Ardoiz, I.; Paton, R. S. GoodVibes: Automated Thermochemistry for Heterogeneous Computational Chemistry Data. *F1000Research* **2020**, *9*, 291.
(78) Zhao, Y.; Truhlar, D. G. The M06 suite of density functionals for main group thermochemistry, thermochemical kinetics, noncovalent interactions, excited states, and transition elements: two new functionals and systematic testing of four M06-class functionals and 12 other functionals. *Theor. Chem. Acc.* **2008**, *120*, 215.
(79) Dolg, M.; Wedig, U.; Stoll, H.; Preuss, H. Energy-adjusted *ab initio* pseudopotentials for the first row transition elements. *J. Chem. Phys.* **1987**, *86*, 866.
(80) Marenich, A. V.; Cramer, C. J.; Truhlar, D. G. Universal Solvation Model Based on Solute Electron Density and on a Continuum Model of the Solvent Defined by the Bulk Dielectric Constant and Atomic Surface Tensions. *J. Phys. Chem. B* **2009**, *113*, 6378.
(81) Legault, C. Y. *CYLview*, ver. 1.0b; Université de Sherbrooke, 2009; http://www.cylview.org.

https://dx.doi.org/10.1021/acscatal.0c02025
ACS Catal. 2020, 10, 8212−8222